Published in final edited form as:
Methods. 2008 November ; 46(3): 204–212. doi:10.1016/j.ymeth.2008.09.009.

Methods for Studying Store-Operated Calcium Entry

Gary S. Bird, **Wayne I. DeHaven**, **Jeremy T. Smyth**, and **James W. Putney Jr.**
Laboratory of Signal Transduction, National Institute of Environmental Health Sciences, National Institutes of Health, Department of Health and Human Services, P. O. Box 12233, Research Triangle Park, North Carolina 27709

Abstract

Activation of surface membrane receptors coupled to phospholipase C results in the generation of cytoplasmic Ca^{2+} signals comprised of both intracellular Ca^{2+} release, and enhanced entry of Ca^{2+} across the plasma membrane. A primary mechanism for this Ca^{2+} entry process is attributed to store-operated Ca^{2+} entry, a process that is activated by depletion of Ca^{2+} ions from an intracellular store by inositol 1,4,5-trisphosphate. Our understanding of the mechanisms underlying both Ca^{2+} release and store-operated Ca^{2+} entry have evolved from experimental approaches that include the use of fluorescent Ca^{2+} indicators and electrophysiological techniques. Pharmacological manipulation of this Ca^{2+} signaling process has been somewhat limited; but recent identification of key molecular players, STIM and Orai family proteins, has provided new approaches. Here we describe practical methods involving fluorescent Ca^{2+} indicators and electrophysiological approaches for dissecting the observed intracellular Ca^{2+} signal to reveal characteristics of store-operated Ca^{2+} entry, highlighting the advantages, and limitations, of these approaches.

I. Introduction

In many cell types, activation of hormone, neurotransmitter, or growth factor receptors coupled to phospholipase-C results in the breakdown of phosphatidylinositol 4,5-bisphoshate, resulting in production of inositol 1,4,5-trisphosphate (IP_3) which stimulates a Ca^{2+} signaling process that is biphasic [1,2]. This biphasic response involves the release of Ca^{2+} ions from an intracellular organelle, the endoplasmic reticulum (ER) or a specialized component of the ER, followed by the entry of Ca^{2+} ions across the plasma membrane. Much is known about the first phase of intracellular Ca^{2+} release from an intracellular organelle, an effect mediated by IP_3 acting on its own receptor, the IP_3 receptor [3]. Until recently, however, the mechanisms regulating the Ca^{2+} entry process have been less well understood, although there is a basic and well established concept for this second phase of Ca^{2+} entry. That is, the degree of emptying of the Ca^{2+}-storage organelle, generated by intracellular Ca^{2+} release, initiates a retrograde signaling process that regulates the rate of Ca^{2+} entry across the plasma membrane. This process is known as capacitative Ca^{2+} entry or store–operated Ca^{2+} entry (SOCE) [4]. The signaling processes underlying SOCE have been the subject of intense study for more than 20 years, yet only recently have the key molecular components been identified. Stim family proteins (Stim1 and 2), appear to function as Ca^{2+} sensors within the ER, and Orai family

Correspondence should be addressed to: Gary S. Bird, NIEHS, P. O. Box 12233, Research Triangle Park, NC 27709. Phone: (919) 541-0214, Fax: (919) 541-1898, Email: bird@niehs.nih.gov.

proteins (Orai1, 2 and 3, also known as CRACM1, 2 and 3) function as SOC channels in the plasma membrane (for recent reviews, see [5,6,7,8]).

Identification of the molecular makeup of the SOCE pathway has been facilitated by optical techniques utilizing fluorescent Ca^{2+} indicators [9,10]. Although the primary focus of this volume is optical techniques, for the study of Ca^{2+} influx mechanisms it is almost always advisable to combine the use of fluorescent indicators with electrophysiological techniques, and these will be discussed in this review as well. In developing these methodological approaches it is important to discriminate SOCE from other pathways that may influence $[Ca^{2+}]_i$. For example, additional mechanisms initiated by phospholipase C activation that can regulate Ca^{2+} entry not related to SOCE have been reported in non-excitable cells [11].

II. Fluorescence-based Measurements of SOCE

Fluorescence-based measurements of $[Ca^{2+}]_i$ have provided a robust and widely used technique for monitoring Ca^{2+} signaling processes, including SOCE. These fluorescence based techniques have been productive due to the availability of a broad range of Ca^{2+} indicators that can be easily introduced into intact cells, and an extensive range of 'turnkey' equipment for measuring Ca^{2+} with good temporal and spatial resolution.

A. Fluorescent Ca^{2+} Indicator Selection

The choice of fluorescent Ca^{2+} indicator is the foundation for a successful study of Ca^{2+} signaling. It can influence the spatial and temporal information that one can collect, and the choices one has for analyzing a response. This selection will also be influenced by the available equipment for measuring fluorescence, such as excitation wavelength selection.

Single Wavelength and Ratiometric Ca^{2+} Indicators—The working core of a Ca^{2+} indicator is centered around its ability to reversibly bind Ca^{2+} ions, with affinities that lie within the physiological range of cytoplasmic $[Ca^{2+}]_i$. With most Ca^{2+} indicators, such as fluo dyes, the level of $[Ca^{2+}]_i$ can be directly monitored as a change in fluorescence intensity of the indicator where, usually, elevation of $[Ca^{2+}]_i$ leads to higher intensity of fluorescence at a single wavelength (Fig.1) . Alternatively, there are some Ca^{2+} indicators that exhibit a spectral shift upon binding Ca^{2+} ions [12] such as the Indo and fura dyes (Fig.1). Using spectral shift indicators has the enormous advantage of providing ratiometric $[Ca^{2+}]_i$ measurements that are independent of the concentration of the Ca^{2+} indicator present in the cells.

Ca^{2+} Binding Affinity and Ion Selectivity—Different Ca^{2+} indicator dyes bind Ca^{2+} with different affinities, and Ca^{2+} affinity is therefore an important consideration when choosing a dye. For example, for most experimental situations fura-5F has proven a useful, if not better, choice than fura-2 for measuring cytoplasmic $[Ca^{2+}]_i$. A derivative of fura-2, fura-5F is handled in exactly the same way in terms of cell loading and recording of fluorescence signals. However, fura-5F has a higher K_D than fura-2 (400 nM vs. 140 nM, respectively), and given that most Ca^{2+} studies examine $[Ca^{2+}]_i$ in the 100 nM – 1 μM range, the advantages of the higher K_D indicator are obvious. The characteristics of fura-5F are shown in Fig.1 and tables 1 and 2, as are those of another commonly used single wavelength Ca^{2+} indicator, fluo-4.

While it may seem intuitive that a Ca^{2+} indicator should be selected based on its selectivity for Ca^{2+} ions over other cations, the ability of these indicators to interact with other cations can provide experimental flexibility for studying Ca^{2+} signaling and SOCE. This has been particularly useful with cations such as Mn^{2+} and Ba^{2+} which, in addition to their ability to interact with Ca^{2+} indicators, can also substitute for Ca^{2+} ions in a number of biological processes, or pharmacologically interfere with these same processes (Table 2). Thus, experimental approaches can be designed that involve substituting alternative cations for

Ca^{2+} ions and these approaches may then reveal specific aspects of the underlying Ca^{2+} signaling process. This has been a particularly useful approach with the fura-based Ca^{2+} indicators and substituting Mn^{2+} [13] or Ba^{2+} [14,15] for Ca^{2+} ions (see below).

Introduction of Ca^{2+} Indicators into Cells—Since Ca^{2+} indicators are charged molecules and do not freely cross biological membranes, a critical factor for ensuring their successful application to biological systems was developing a way to load the indicator into the cytoplasm of intact cells. Fortunately, an innovative approach was developed whereby charged residues were chemically masked with acetoxy methyl ester groups (AM groups) [16]. The uncharged products cross the plasma membrane into the cytoplasm where non-specific esterases cleave the AM groups leaving the charged and Ca^{2+}-sensitive form of the indicator to accumulate in that cell compartment.

One complicating problem associated with AM derivatives of Ca^{2+} indicators is that their accumulation may not be restricted to the cell cytoplasm. That is, the AM derivative may cross other membranes and accumulate in compartments such as the ER and mitochondria. The extent of this compartmentalization can vary depending on the type of cell being used. For example, no such problem is apparent with HEK 293 cells, whereas it presents a major obstacle in primary rat hepatocytes [17]. Fortunately, there are ways to diagnose and minimize this problem. Diagnosis can include: (i) A non-uniform and punctate spatial distribution of the Ca^{2+} indicator; (ii) Calibrated Ca^{2+} indicator values indicative of high resting cytoplasmic $[Ca^{2+}]_i$; (iii) Poor or lack of agonist-induced $[Ca^{2+}]_i$ response; (iv) A combination of agonist and a sarco-endoplasmic reticulum Ca^{2+}-ATPase (SERCA)-pump inhibitor (thapsigargin) leads to a drop in resting cytoplasmic $[Ca^{2+}]$ levels (See [17,18]). Minimizing compartmentalization can usually be achieved by manipulating indicator concentration, duration of incubation with AM-indicator, and the temperature of the incubation. In the event that compartmentalization cannot be resolved, one has the option of introducing free acid forms of Ca^{2+} indicators directly into the cytoplasm by techniques such as microinjection or electroporation [17,19].

Leakage of Ca^{2+} indicators out of the intact cell is an additional complication with contributing factors including the specific Ca^{2+} indicator choice and/or the cell type being used. In some instances, the problem appears due to the Ca^{2+} indicator being a substrate for organic anion transporters, an effect that can be minimized by including anion transport inhibitors such as probenicid and sulfinpyrazone in all experimental solutions [20].

Data Representation—Due to the non-linear relationship between Ca^{2+} indicator fluorescence changes and $[Ca^{2+}]_i$, calibration of the fluorescence signal [12] is advisable for instances such as looking for subtle quantitative effects on $[Ca^{2+}]_i$ signaling, or as a means to compare experimental data collected from different instrumentation. However, in many instances a general understanding of $[Ca^{2+}]_i$ signaling mechanisms such as SOCE can be gleaned from fluorescence intensities or fluorescence ratios. If uncalibrated ratios are used it is minimally recommended that you (i) ensure the Ca^{2+} indicator used has an appropriate affinity to maximize the dynamic range of the measurement and avoid the possibility of saturating the indicator, and (ii) correct data for fluorescence signals not related to Ca^{2+}-sensitive fluorescence changes (auto-fluorescence), which minimizes cell-to-cell variation as well as variability between experiments.

In the case of ratiometric fura dyes, auto-fluorescence is readily estimated by quenching fura dyes with Mn^{2+} ions (treat cells with ionomycin and $MnCl_2$, 10 μM and 20 mM, respectively, in a nominally Ca^{2+}-free bathing solution). Single wavelength indicators like fluo-4 and Calcium Green-1 are not completely quenched by Mn^{2+}, thus non-indicator loaded cells may provide an estimation of autofluorescence.

B. Quantitative Assessment of SOCE

Activating SOCE: SERCA Inhibitors/Ca^{2+}-Ionophores—As described above, depletion of intracellular Ca^{2+}-stores located within the ER plays a key role in activating SOCE and is primarily achieved through IP_3-induced Ca^{2+}-mobilization during agonist activation. The ER also serves as a critical Ca^{2+}-buffer, with Ca^{2+}-ATPases (SERCA pumps) that can rapidly sequester Ca^{2+} ions from the cell cytoplasm to prevent untoward changes in $[Ca^{2+}]_i$ and replenish ER Ca^{2+}-stores following agonist activation. Even in unstimulated cells, Ca^{2+} ions are continually cycling across the ER membrane with the actions of SERCA pumps sequestering Ca^{2+} balanced against a poorly defined 'Ca^{2+} leak' process out of the ER (but see [21,22]). Fortunately, there are a number of pharmacological reagents that target and inhibit the function of the SERCA Ca^{2+}-pumps and, with the 'Ca^{2+} leak' process in effect, results in depletion of ER Ca^{2+}-stores and full activation SOCE (Fig.2B).

Discovery of SERCA inhibitors, namely thapsigargin, cyclopiazonic acid (CPA) and tBHQ [23] provided an important validation of the SOCE model of Ca^{2+} entry, especially as these reagents made it possible to deplete the IP_3-sensitive Ca^{2+} stores and activate SOCE without formation of any inositol phosphates associated with agonist activation [24]. SERCA pump inhibitors are membrane permeant, and provide a non-invasive technique for manipulating ER Ca^{2+}-pools and SOCE activation in intact cells. Activating SOCE with thapsigargin is, however, a difficult process to reverse. In contrast, CPA is more water soluble than thapsigargin, and appears more amenable to washing out of cells, and offers the possibility of achieving partial depletion of intracellular Ca^{2+} stores with a range of CPA concentrations, resulting in partial activation of SOCE [25].

An alternative to SERCA pump inhibition is to deplete ER Ca^{2+}-pools using a Ca^{2+}-ionophore such as ionomycin [26]. A carboxylic acid antibiotic, ionomycin is a mobile ion carrier that has proven effective in manipulating the movement of Ca^{2+} ions and intracellular Ca^{2+}-pools in intact cells. Low concentrations of ionomycin (<1μM) appear to selectively release intracellular Ca^{2+}-stores (ED_{50} = 50 nM) without directly increasing the permeability of the plasma membrane to extracellular Ca^{2+} [27,28]. At higher concentrations (1-10 μM), the ionophore increases the permeability of the plasma membrane, ER and mitochondria to Ca^{2+} ions.

In general, ionomycin is preferred over A23187 since, with fluorescent Ca^{2+} indicators excited in the UV range, A23187 can contribute significant autofluorescence to the measured signal (a non-fluorescent derivative, 4Br-A23187, is available [29].

'Ca^{2+} Re-Addition' Protocol: Dissecting out SOCE—In unstimulated cells, the concentration of Ca^{2+} ions in the cytoplasm (~10^{-7} M) reflects a steady state balance of homeostatic mechanisms involving Ca^{2+} pumps and channels. Cells utilize ATP-dependent Ca^{2+} pumps to maintain this level against a background of enormous Ca^{2+} gradients (extracellular milieu ~10^{-3} M; ER ~10^{-4} M). In addition in most, but not all cell types, plasma membrane permeability to Ca^{2+} is very low unless altered by a physiological or pathological mechanism. Figure 2A illustrates a principle method for disrupting steady state $[Ca^{2+}]_i$ conditions by simply modifying extracellular Ca^{2+} conditions ($[Ca^{2+}]_o$). In this 'Ca^{2+} re-addition' protocol, the salt solution bathing cells is switched alternatively from one containing normal $[Ca^{2+}]_o$ (1-2 mM) to a salt solution that is depleted or nominally Ca^{2+}-free, and then back again to normal $[Ca^{2+}]_o$ conditions. Depending on the water source and purity of salts used, nominally Ca^{2+}-free buffers can contain $[Ca^{2+}]$ in the range of a few μM. Alternatively, one can ensure the solutions are Ca^{2+}-free by supplementing them with a Ca^{2+}-chelator such as EGTA or BAPTA (100-500 μM). As shown in Fig. 2A for an unstimulated HEK 293 cell loaded with fura-5F, the Ca^{2+} re-addition protocol does not result in any detectable change in $[Ca^{2+}]_i$ (this is not always the case, for example see [30]). Characterizing this response in

unstimulated cells is an important control to characterize the cell type being used and the full extent of SOCE activation measured in stimulated cells. In Fig.2B, the 'Ca^{2+} re-addition' protocol is now used in the same fura-5F-loaded HEK 293 cells, but this time treated with thapsigargin to empty Ca^{2+} stores and thus fully activate SOCE. In the absence of extracellular Ca^{2+}, thapsigargin treatment results in a $[Ca^{2+}]_i$ response that is transient, representing the release of Ca^{2+} ions from intracellular Ca^{2+} pools. On adding back extracellular Ca^{2+} to the bathing medium, the second phase of SOCE is revealed resulting in a rise in $[Ca^{2+}]_i$ to an elevated and sustained phase. The cells will remain at this elevated $[Ca^{2+}]_i$ level until the Ca^{2+}-store depletion stimulus is removed, or $[Ca^{2+}]_o$ is modified.

In summary, the basic approach described in the Ca^{2+} re-addition protocol is to separate the two phases of Ca^{2+} mobilization, Ca^{2+} release and SOCE. At the point of restoring $[Ca^{2+}]_o$, manipulations of the bathing solution, including cation substitutions, can enhance or distinguish Ca^{2+}-entry pathways on the basis of their pharmacological properties (see below). An interesting variation of this protocol is a 'Ca^{2+}-overshoot protocol'. In this method, phospholipase C-coupled receptors are transiently activated in the absence of extracellular Ca^{2+}, with Ca^{2+} re-addition occurring after the stimulus is removed. With this protocol, and despite the removal of the cell stimulus, intracellular Ca^{2+} pools remain depleted, and SOCE remains activated until extracellular Ca^{2+} is restored and Ca^{2+} pools refilled. In some cell types, this SOCE activity can be observed as a transient rise in $[Ca^{2+}]_i$, or'Ca^{2+}-overshoot', following Ca^{2+} re-addition [31].

Quantifying SOCE: Peaks and Rates—Three general methods have been used to quantitatively analyze Ca^{2+} influx from experiments such as in Fig. 2C: initial rate of $[Ca^{2+}]_i$ rise, peak $[Ca^{2+}]_i$ level, and area under the $[Ca^{2+}]_i$ curve. In theory at least, initial rates should give the cleanest indication of Ca^{2+} influx, although it is clear that cellular Ca^{2+} buffering occurs so rapidly that even this measure can be influenced by many factors. These factors can sometimes be minimized by the use of Ca^{2+} surrogates such as Ba^{2+} or Mn^{2+}, which do not activate negative feedbacks and are poor substrates for cellular Ca^{2+} buffers. This is discussed in more detail below. Peak responses are probably more commonly reported, but these have the disadvantage that $[Ca^{2+}]_i$ levels are often limited in non-linear ways by cellular feedback mechanisms and Ca^{2+} buffers. Least desirable is the use of integrated areas under the $[Ca^{2+}]_i$ curve; these are generally sustained responses and thus the areas will depend upon arbitrarily selected time intervals, and will to varying degrees be even more affected by secondarily activated pumps and inactivation mechanisms.

Monitoring SOCE with Ca^{2+} Surrogates—The complexity of homeostatic mechanisms that regulate $[Ca^{2+}]_i$ can lead to a number of potential artifacts when using Ca^{2+} ions to monitor SOCE in fluorescence-based experiments. Any mechanism that limits the extent of a $[Ca^{2+}]_i$ rise can result in non-linear behaviors that belie appropriate quantitative analysis. These mechanisms can include activation of plasma membrane pumps to extrude Ca^{2+} ions and/or feedback inhibition of SOC channels. For example, a treatment that inhibits intracellular Ca^{2+}-ATPases (such at thapsigargin) at the same time as activating SOCE may have a quantitatively different effect on elevating $[Ca^{2+}]_i$ compared to SOCE activation by other means. These problems can sometimes by minimized by substituting for Ca^{2+} cations that will permeate through SOC channels but are poor substrates for other Ca^{2+}-dependent enzymes such as Ca^{2+}-pumps. Mn^{2+} or Ba^{2+} have proven very useful substitutes for $[Ca^{2+}]_o$ for SOCE measurements, particularly when using the Ca^{2+} re-addition protocol. However, it should be noted that not all Ca^{2+}-indicators behave in the same way to these Ca^{2+} surrogates (see Table 2).

Mn^{2+} ions appear to traverse most Ca^{2+}-permeable channels [32] and substitute for Ca^{2+} in SOCE [33], despite the fact that CRAC channels are less permeable to Mn^{2+} than to Ca^{2+}

[34]. In fluorescence-based $[Ca^{2+}]_i$ measurements, fura-indicators are ideally suited to monitor Mn^{2+}-entry as they irreversibly bind Mn^{2+} (due to high affinity for the cation), which quenches the fura fluorescence. Quantifying Mn^{2+}-entry can easily be done by monitoring the Mn^{2+}-quench process at fura-2's isobestic wavelength (~360 nm), or by using an algebraic summation of fluorescence values obtained from excitation at two different wavelengths [35]. Thus, activation of SOCE activity can easily be quantified by measuring initial rates of Mn^{2+} quench in fura-loaded cells [36]. In quantifying SOCE activity, it is important to measure basal Mn^{2+}-quench rates in unstimulated cells, since most cells exhibit a basal, constitutive permeability to Mn^{2+}. A useful facet of the Mn^{2+}-quench technique is that you can monitor Ca^{2+}-release events and Mn^{2+}-quench (SOCE) simultaneously [35,37].

There are some limitations with using the Mn^{2+}-quench technique. One is that it is not applicable to all Ca^{2+}-indicators, for example the single wavelength indicator Fluo-4 is poorly responsive to Mn^{2+} ions, and Calcium Green-1 fluorescence intensity is actually increased by Mn^{2+}, not quenched. Another surrounds an artifact when applying Mn^{2+}-quench to cells with significant compartmentalization of fura-indicators in the ER. While Mn^{2+} is not a substrate for intracellular SERCA pumps, it can easily pass through activated IP_3 receptors in a retrograde manner [17]. This presents a problem when monitoring SOCE with agonist stimulation since the observed Mn^{2+}-quench may reflect IP_3 mediated movement into the ER rather than flux across the plasma membrane.

Monitoring Ba^{2+} entry by substituting Ba^{2+} for Ca^{2+} ions in the Ca^{2+} re-addition protocol has provided a useful measure of SOCE [15]. Fura-based indicators are amenable for this technique since Ba^{2+} can substitute for Ca^{2+} and render an excitation spectrum similar to that for Ca^{2+}. Importantly, Ba^{2+} is a poor substrate for Ca^{2+}-pumping ATPases and does not enter ER Ca^{2+}-pools. Thus, monitoring Ba^{2+}-entry during cell activation provides a measure of SOCE activity without complications due to buffering by Ca^{2+}-pumps and Ca^{2+}-pool refilling. As for Mn^{2+}-quench, quantifying initial rates of Ba^{2+} entry is recommended, as well as taking into account basal rates of entry in the absence of cell stimulation. One potential artifact that could be encountered when using Ba^{2+} ions involves altering membrane potential [38], which can influence SOCE activity (see below).

III. Electrophysiological Measurement of SOC Currents

A. Biophysical Characteristics of Store-operated Currents

An understanding of SOCE and its regulation has been facilitated by the electrophysiological characterization of plasma membrane Ca^{2+} currents associated with SOCE. The most extensively studied and most thoroughly characterized store-operated current was first identified in mast cells as Ca^{2+} release-activated Ca^{2+} current, or I_{crac} [39,34]. I_{crac} is a small current, often below the level of reliable detection. It is largest in hematopoetic cells where it can be up to 2 pA/pF, under optimal recording conditions. But for many cell types, the measurement of store-operated entry by electrophysiological means has not always been a practical approach since the currents apparently fall near or below the limits of detection. For instance, in HEK293 cells the store-operated Ca^{2+} current is maximally only about 0.5 pA/pF. This limitation can be circumvented to some extent by carrying out experiments under conditions where cells are maintained in an extracellular solution that is divalent cation-free (DVF, see below). Studies on I_{crac}, indicate that the underlying channels have a small pore diameter [40], low permeability to Cs^+, and an extremely small unitary conductance for Ca^{2+} and Na^+ [34,41,40,42,43]. While no single channel events have been detected for I_{crac}, fluctuation analysis predicts a monovalent unitary conductance of less than 1 pS [40].

B. Biophysical Assessment of Store-operated Currents

Electrophysiological measurement of I_{crac} is usually carried out in whole-cell patch clamp mode (Fig.3A). This mode offers a number of experimental advantages, in particular the ability to define and control the conditions bathing the intracellular and extracellular milieu, and to precisely control membrane potential. With fluorescence-based $[Ca^{2+}]_i$ measurements on SOCE, the inability to control membrane potential in intact cells is a problem that can potentially give rise to experimental artifacts (see below for discussion).

General protocols to record I_{crac} using the whole-cell patch-clamp technique are reviewed in [4]. This technique involves the establishment of a tight seal between a recording pipette electrode and the surface membrane of a cell, followed by rupture of the membrane under the pipette opening to establish electrical and chemical continuity between the pipette and the cytoplasm (Fig 3A). This then allows the cell membrane potential to be clamped (usually at a depolarized potential, 0 mV) until, every 1 to 2 seconds, a voltage ramp is applied from -100 mV up to +100 mV (see Fig. 3B). With this protocol, the measured currents can reveal how I_{crac} develops over time (Fig. 3C) as well as its current-voltage relationship which, for I_{crac}, is inwardly rectifying (Fig. 3D). After completing each voltage ramp, it is routine to return to the depolarized potential (0 mV). This is an important step in the protocol as it reduces the driving force for Ca^{2+} ions entering the cell, and thus lessens Ca^{2+} dependent feedback pathways that inactivate CRAC channels.

Figure 3C illustrates a typical experiment utilizing RBL cells in the whole-cell configuration to measure I_{crac} activation. After break-in and establishing a whole cell patch, the cell was held at 0 mV followed by applying a voltage ramp from -100 mV to +100 mV every 2 seconds. The internal pipette solution (described in Table 3) contained IP_3 (20 μM) and BAPTA (10 mM), optimal conditions to rapidly deplete ER Ca^{2+} stores and activate SOCE. The extracellular bathing solution (described in Table 3) contained 10 mM Ca^{2+}. Over a period of seconds after break-in, a small inward current can be observed developing at -100 mV, while little to no change is detected at +100 mV. Plotting the current-voltage relationship of this data (Fig. 3D; please note that these figures have been leak subtracted) clearly demonstrates that I_{crac}, activated by Ca^{2+} store depletion, is strongly inwardly rectifying.

An important characteristic of the CRAC channel is that it completely loses its Ca^{2+} selectivity when all extracellular divalent cations are removed, and Na^+ ions are now allowed to permeate the channel. So under extracellular divalent free (DVF) conditions (see table 3), CRAC channel activity can now be measured as a function of current carried by Na^+ ions. Interestingly, Na^+ currents carried through CRAC channels (Na^+-I_{crac}) run down over time by a process known as *depotentiation*, which is the reciprocal of a process known as Ca^{2+} dependent potentiation (see below).

Critically, the Na^+-I_{crac} current densities measured under DVF conditions are large, and has provided an invaluable technique for characterizing SOC channels in cells where there is little to no detectable Ca^{2+}-I_{crac} (I_{crac} measured with divalent cations present in extracellular solutions) (Fig. 3E, and examples in [44,45]). However, it is advisable that the Na^+ currents recorded be characterized pharmacologically to ensure that they represent the activity of CRAC channels (see below).

C. Activating Store-operated Currents

The single initial signal for the activation of SOCE and I_{crac} is the depletion of intracellular Ca^{2+} stores located in the ER. As mentioned above, I_{crac} activation is measured using the whole-cell patch, allowing the intracellular milieu to be modified directly with the internal patch pipette solution. Thus, rather than relying of the actions of SERCA pump inhibitors like

thapsigargin or ionomycin (both added to extracellular solution) to activate SOC channels, intracellular Ca^{2+} store depletion can be achieved by additions to the internal pipette solution.

The simplest mode of I_{crac} activation is through '*passive depletion*' of intracellular Ca^{2+} stores. By simply breaking into cells with a patch pipette solution containing a high concentration of BAPTA or EGTA and no added Ca^{2+} (see table 3), the intracellular Ca^{2+} stores are gradually lost. This technique is at least in principle equivalent to the use of SERCA inhibitors. The passive process is slow, and I_{crac} activation may take in the order of several minutes to fully develop (Fig.4A). Alternatively, one can use the whole-cell patch clamp technique to introduce membrane impermeant reagents to actively and rapidly deplete intracellular Ca^{2+} stores and activate I_{crac}. The most efficient way is to include metabolizable or non-metabolizable analogs of IP_3 (in conjunction with EGTA or BAPTA) [46]. Under these conditions, the time course of I_{crac} activation is significantly faster than with passive depletion alone (Fig.4A).

Ca^{2+}-dependent feedback regulation of I_{crac}—I_{crac} is both positively and negatively regulated by Ca^{2+} in a complex manner. First, Ca^{2+} regulates SOC channels in a positive manner through a process known as Ca^{2+} dependent potentiation (CDP) [47,48], and appears to result from Ca^{2+} ions interacting with an extracellular binding site. While this binding site has not been identified as yet, it is possible that it is the same as the Ca^{2+} binding site in the selectivity filter. Nonetheless, the presence of Ca^{2+} at this putative CDP site potentiates I_{crac}, and can be detected electrophysiologically when switching between external DVF solution and Ca^{2+} containing (10 mM) solutions. As mentioned above, the reverse of CDP can be detected when switching from a Ca^{2+} containing extracellular solution to DVF solutions to detect Na^+I_{crac}, the effect being that the Na^+ current depotentiates (Figure 3C and 3E).

Under conditions whereby $[Ca^{2+}]_i$ levels are high in close proximity to the CRAC channels, CRAC channels can experience two types of Ca^{2+}-dependent feedback regulation described as either *fast* or *slow inactivation* [34,49,50,51]. Fast inactivation of I_{crac} can be observed electrophysiologically by using brief hyperpolarizing steps from depolarized holding potentials (for protocol, see [34,49,51]), and is believed to result from Ca^{2+} entering through the channels binding directly to the channels at or near the channel mouth. This effect occurs in the millisecond time range, and differences in the rates of fast inactivation can be seen by comparing the effects of the slower Ca^{2+} chelator EGTA with the faster chelator, BAPTA [34,49,51] in the internal pipette solution.

In contrast, slow inactivation of I_{crac} occurs over a period of tens of seconds [52,50,53]. While the mechanism underlying slow inactivation is not fully understood, slow inactivation might occur due to refilling of intracellular Ca^{2+} stores and could occur if cytoplasmic $[Ca^{2+}]_i$ levels were significantly elevated in spatially restricted areas and thus locally overwhelmed the Ca^{2+} chelator included in the internal pipette solution. Alternatively, slow inactivation might be due to a regulatory feedback mechanism on the SOCE signaling process, for example it has been suggested that PKC regulates I_{crac} activity [52].

In summary, feedback regulation of I_{crac} by Ca^{2+} ions is a complex multitude of processes that are yet to be fully defined. While these Ca^{2+} signaling pathways may play crucial roles in the physiology of many cells types, awareness of these processes is crucial for studying SOC channels electrophysiologically and for understanding how they can be controlled experimentally.

IV. Manipulating SOCE

Cytoplasmic $[Ca^{2+}]_i$ reflects a homeostatic balance of Ca^{2+} pumps and Ca^{2+} channel activities. Any disturbance in these processes, through receptor-dependent activation of Ca^{2+} channel

activity for example, can lead to the rapid movement of Ca^{2+} down concentration gradients until a new steady state is achieved in concert with Ca^{2+} pump and feedback mechanisms. Experimental manipulations and pharmacological agents that interfere with any of these Ca^{2+} homeostatic processes can have a profound effect on the cytoplasmic $[Ca^{2+}]_i$ and plasma membrane currents. Thus, an intimate understanding of the underlying Ca^{2+} homeostatic processes and the various ways they can be manipulated will allow the observed fluorescence-based $[Ca^{2+}]_i$ signals and membrane currents to be interpreted in meaningful ways that speak to the underlying Ca^{2+} signaling process. Some of these approaches are outlined below.

A. Pharmacological Manipulation of SOCE

Pharmacological manipulation of SERCA pumps with inhibitors such as thapsigargin was crucial for developing our understanding of SOCE (see above). Unfortunately, our ability to manipulate SOC channels directly and inhibit them with any degree of specificity has been rather limited. Amongst the arsenal of tools proposed as SOC channel inhibitors [23,4], lanthanides and 2-aminoethyldiphenyl borate (2-APB) have proven most useful in manipulating SOC entry, with lanthanides appearing to be the most selective (see below).

Due to their physical chemistry [54], lanthanides were exploited as tools to block both Ca^{2+} entry and efflux processes [55]. Fortunately, SOCE is much more sensitive to inhibition by lanthanides than Ca^{2+}-efflux across the plasma membrane. The lanthanide Gd^{3+} is generally used in this respect and appears specific for SOCE over non-SOCE pathways when used in the appropriately low ($\leq$5 μM) concentration range [56], and only begins to block PMCA activity above 100 μM [57].

When using this approach, care should be taken to use freshly prepared lanthanide salt solutions in buffers devoid of divalent anions. Also the presence of extracellular BAPTA or EGTA will bind lanthanides with high affinity [56] and adversely affect their concentration in solution. Another potential problem stems from the ability of lanthanides to render an excitation spectrum with fura-based Ca^{2+}-indicators. Usually, lanthanides poorly traverse the plasma membrane of intact cells, if at all [15]. However, should bathing an unstimulated cell with a lanthanide increase the fura-signal, this could be indicative of ‘leaky’ or unhealthy cells.

2-APB has proven a somewhat selective inhibitor for SOCE [58,59,60,61,62], an effect that appears to be extracellular at the plasma membrane [59,61,63,64], and independently of IP_3 receptor inhibition [65]. However, a careful evaluation of 2-APB effects on Ca^{2+}-signaling processes is advised. Originally shown to be a membrane permeable inhibitor of IP_3 receptors [66], the effects of 2-APB are proving complex and this drug may lack the desired specificity. These effects can include inhibiting a magnesium-inhibitable cation channel [59,43], or activating distinct ion channel activity depending on the concentration of 2-APB [67,68,69].

B. Membrane Potential

Contrary to voltage-activated Ca^{2+} channels, membrane depolarization does not play a role in SOCE activation. However, since Ca^{2+} entry through SOC channels is an electrogenic process driven by chemical (concentration gradient) and electrical (membrane potential) forces, plasma membrane potential can regulate SOCE such that less Ca^{2+} enters upon depolarization and membrane hyperpolarization promotes Ca^{2+} influx [70,71].

Membrane potential is well controlled when using voltage-clamp techniques to measure SOC channel activity (see below). However, when measuring SOCE with fluorescent Ca^{2+}-indicators alone, changes in membrane potential are usually not controlled, but it is possible to carry out fluorescence measurements of $[Ca^{2+}]_i$ under voltage clamped conditions [72]. Lack of control of membrane potential must be considered when characterizing pharmacological

agents that affect SOCE [73], since modulation of the Ca^{2+}-entry signal could result from depolarization/hyperpolarization rather than direct effects on the SOC channel itself.

Monitoring membrane potential and characterizing the effects of candidate pharmacological agents for SOCE is one way to control for this. Alternatively, these complications can be avoided by combining voltage-clamp techniques with fluorescence Ca^{2+} measurements. If this option is not available, one can manipulate the bathing solution to contain high [KCl] and create a "poor man's voltage-clamp" and carry out fluorescence experiments with the plasma membrane fully depolarized [74,75,76].

C. Manipulating the Molecular Players for SOCE

As described above, the main limitation to developing approaches that specifically manipulate SOCE has been our poor understanding of the molecular players involved in this process. Fortunately, the recent identification of STIM and Orai (or CRACM) family proteins has facilitated our understanding of the target plasma membrane channel mediating SOCE, as well as the mechanism by which depletion of intracellular Ca^{2+} stores is communicated to these SOC channels at the plasma membrane [77].

These discoveries have opened new experimental approaches to dissect and manipulate SOCE through techniques such as RNAi [78,79,80,81,82,83], protein modification and expression [84], and the generation of animal models [45]. These approaches have enabled structure function studies on Orai family proteins to identify residues involved in pore formation and the selectivity filter [85,86,87]. These studies may very well lay the foundation to develop new pharmacological strategies to manipulate SOCE [88].

V. Concluding Remarks

The purpose of this review is to delineate useful strategies for dissecting Ca^{2+} signaling processes and studying SOCE using experimental approaches that employ fluorescent Ca^{2+} indicators and electrophysiological techniques. The ability to use these diverse experimental approaches to monitor $[Ca^{2+}]i$ and SOC currents in real time, with varying degrees of spatial and temporal resolution, has significantly contributed to our current understanding of the basic processes of regulated SOCE.

It remains a challenge to continually refine protocols and experimental conditions to optimally discriminate SOCE from other possible routes of Ca^{2+}-entry across the plasma membrane. This is especially important when identifying a role for SOCE under conditions of physiological activation of phospholipase C-linked pathways and SOCE, or in considering a role for SOCE in excitable cells. The identification of the molecular players for SOCE, STIM and Orai family proteins, has also opened up exciting possibilities to derive new strategies to specifically manipulate SOCE, as well as delineate all the steps involved in this Ca^{2+} signaling pathway.

Reference List

1. Putney JW, Poggioli J, Weiss SJ. Phil Trans R Soc Lond B 1981;296:37–45. [PubMed: 6121344]
2. Berridge MJ, Irvine RF. Nature 1984;312:315–321. [PubMed: 6095092]
3. Berridge MJ. Ann Rev Biochem 1987;56:159–193. [PubMed: 3304132]
4. Parekh AB, Putney JW. Physiol Rev 2005;85:757–810. [PubMed: 15788710]
5. Cahalan MD, Zhang SL, Yeromin AV, Ohlsen K, Roos J, Stauderman KA. Cell Calcium 2007;42:133–144. [PubMed: 17482674]
6. Vig M, Kinet JP. Cell Calcium 2007;42:157–162. [PubMed: 17517435]
7. Gwack Y, Feske S, Srikanth S, Hogan PG, Rao A. Cell Calcium 2007;42:145–156. [PubMed: 17572487]

8. Lewis RS. Nature 2007;446:284–287. [PubMed: 17361175]
9. Tsien RY. Annual Review of Neuroscience 1989;12:227–253.
10. Vorndran C, Minta A, Poenie M. Biophysical Journal 1995;69:2112–2124. [PubMed: 8580355]
11. Shuttleworth TJ, Thompson JL. The Biochemical Journal 1996;316:819–824. [PubMed: 8670157]
12. Grynkiewicz G, Poenie M, Tsien RY. Journal of Biological Chemistry 1986;260:3440–3450. [PubMed: 3838314]
13. Hallam TJ, Jacob R, Merritt JE. The Biochemical Journal 1988;255:179–184. [PubMed: 3196311]
14. Almers W, McCleskey EW. J Physiol 1984;353:585–608. [PubMed: 6090646]
15. Kwan CY, Putney JW. Journal of Biological Chemistry 1990;265:678–684. [PubMed: 2404009]
16. Tsien RY. Nature 1981;290:527–528. [PubMed: 7219539]
17. Glennon MC, Bird GStJ, Kwan C-Y, Putney JW. Journal of Biological Chemistry 1992;267:8230–8233. [PubMed: 1533221]
18. Glennon MC, Bird GS, Takemura H, Thastrup O, Leslie BA, Putney JW. J Biol Chem 1992;267:25568–25575. [PubMed: 1460052]
19. Quintana A, Hoth M. Cell Calcium 2004;36:99–109. [PubMed: 15193858]
20. Di Virgilio F, Steinberg TH, Silverstein SC. Cell Calcium 1990;11:57–62. [PubMed: 2191781]
21. Lomax RB, Camello C, Van Coppenolle F, Petersen OH, Tepikin AV. Journal of Biological Chemistry 2002;277:26479–26485. [PubMed: 11994289]
22. Ong HL, Liu X, Sharma A, Hegde RS, Ambudkar IS. Pflugers Archiv European Journal of Physiology. 2006
23. Putney JW. Mol Interventions 2001;1:84–94.
24. Takemura H, Hughes AR, Thastrup O, Putney JW. Journal of Biological Chemistry 1989;264:12266–12271. [PubMed: 2663854]
25. Sedova M, Klishin A, Hüser J, Blatter LA. J Physiol (Lond) 2000;523:549–559. [PubMed: 10718737]
26. Liu C-M, Herman TE. Journal of Biological Chemistry 1979;253:5892–5894. [PubMed: 28319]
27. Albert PR, Tashjian AH Jr. Journal of Biological Chemistry 1984;259:15350–15363. [PubMed: 6439720]
28. Morgan AJ, Jacob R. The Biochemical Journal 1994;300:665–672. [PubMed: 8010948]
29. Deber CM, Tom-Kun J, Mack E, Grinstein S. Anal Biochem 1985;146:349–352. [PubMed: 3927770]
30. Bird, GStJ; Takemura, H.; Thastrup, O.; Putney, JW.; Menniti, FS. Cell Calcium 1991;13:49–58. [PubMed: 1371721]
31. Takemura H, Putney JW. The Biochemical Journal 1989;258:409–412. [PubMed: 2650680]
32. Anderson A. Journal of General Physiology 1983;81:805–827. [PubMed: 6308126]
33. Hallam TJ, Rink TJ. FEBS Letters 1985;186:175–179. [PubMed: 2408921]
34. Hoth M, Penner R. J Physiol (Lond) 1993;465:359–386. [PubMed: 8229840]
35. Shuttleworth TJ. Cell Calcium 1994;15:457–466. [PubMed: 8082129]
36. Chiavaroli C, Bird GStJ, Putney JW. Journal of Biological Chemistry 1994;269:25570–25575. [PubMed: 7523388]
37. Loessberg PA, Zhao H, Muallem S. Journal of Biological Chemistry 1991;266:1363–1366. [PubMed: 1899088]
38. Franchini L, Levi G, Visentin S. Cell Calcium 2004;35:449–459. [PubMed: 15003854]
39. Hoth M, Penner R. Nature 1992;355:353–355. [PubMed: 1309940]
40. Prakriya M, Lewis RS. J Gen Physiol 2006;128:373–386. [PubMed: 16940559]
41. Bakowski D, Parekh AB. Cell Calcium 2002;32:379–391. [PubMed: 12543097]
42. Prakriya M, Lewis RS. Cell Calcium 2003;33:311–321. [PubMed: 12765678]
43. Prakriya M, Lewis RS. Journal of General Physiology 2002;119:487–507. [PubMed: 11981025]
44. DeHaven WI, Smyth JT, Boyles RR, Putney JW. J Biol Chem 2007;282:17548–17556. [PubMed: 17452328]
45. Vig M, DeHaven WI, Bird GS, Billingsley JM, Wang H, Rao PE, Hutchings AB, Jouvin MH, Putney JW, Kinet JP. Nat Immunol 2008;9:89–96. [PubMed: 18059270]

46. Parekh AB, Penner R. Physiological Reviews 1997;77:901–930. [PubMed: 9354808]
47. Christian EP, Spence KT, Togo JA, Dargis PG, Patel J. J Membrane Biol 1996;150:63–71. [PubMed: 8699480]
48. Zweifach A, Lewis RS. Journal of General Physiology 1996;107:597–610. [PubMed: 8740373]
49. Zweifach A, Lewis RS. Journal of General Physiology 1995;105:209–226. [PubMed: 7760017]
50. Zweifach A, Lewis RS. Journal of Biological Chemistry 1995;270:14445–14451. [PubMed: 7540169]
51. Fierro L, Parekh AB. J Membr Biol 1999;168:9–17. [PubMed: 10051685]
52. Parekh AB, Penner R. Proceedings of the National Academy of Sciences USA 1995;92:7907–7911.
53. Parekh AB. Journal of Biological Chemistry 1998;273:14925–14932. [PubMed: 9614097]
54. Lettvin JY, Pickard WF, MCCULLOCH WS, PITTS W. Nature 1964;202:1338–1339. [PubMed: 14210975]
55. Van Breemen C, Farinas B, Gerba P, McNaughton ED. Circulation Research 1972;30:44–54. [PubMed: 5007527]
56. Broad LM, Cannon TR, Taylor CW. J Physiol (Lond) 1999;517:121–134. [PubMed: 10226154]
57. Bird GS, Putney JW. J Physiol 2005;562:697–706. [PubMed: 15513935]
58. Ma H-T, Patterson RL, van Rossum DB, Birnbaumer L, Mikoshiba K, Gill DL. Science 2000;287:1647–1651. [PubMed: 10698739]
59. Braun F-J, Broad LM, Armstrong DL, Putney JW. Journal of Biological Chemistry 2001;276:1063–1070. [PubMed: 11042187]
60. Gregory RB, Rychkov G, Barritt GJ. The Biochemical Journal 2001;354:285–290. [PubMed: 11171105]
61. Bakowski D, Glitsch MD, Parekh AB. J Physiol (Lond) 2001;532:55–71. [PubMed: 11283225]
62. Bootman MD, Collins TJ, Mackenzie L, Roderick HJ, Berridge MJ, Peppiatt CM. The FASEB Journal 2002;16:1145–1150. [PubMed: 12153982]
63. Prakriya M, Lewis RS. J Physiol (Lond) 2001;536:3–19. [PubMed: 11579153]
64. Iwasaki H, Mori Y, Hara Y, Uchida K, Zhou H, Mikoshiba K. Receptors and Channels 2001;7:429–439. [PubMed: 11918346]
65. Broad LM, Braun F-J, Lièvremont J-P, Bird GStJ, Kurosaki T, Putney JW. Journal of Biological Chemistry 2001;276:15945–15952. [PubMed: 11278938]
66. Maruyama T, Kanaji T, Nakade S, Kanno T, Mikoshiba K. Journal of Biochemistry 1997;122:498–505. [PubMed: 9348075]
67. Braun FJ, Aziz O, Putney JW. Molecular Pharmacology 2003;63:1304–1311. [PubMed: 12761340]
68. Chung MK, Lee H, Mizuno A, Suzuki M, Caterina MJ. Journal of Neuroscience 2004;24:5177–5182. [PubMed: 15175387]
69. Hu HZ, Gu Q, Wang C, Colton CK, Tang J, Kinoshita-Kawada M, Lee LY, Wood JD, Zhu MX. Journal of Biological Chemistry 2004;279:35741–35748. [PubMed: 15194687]
70. Merritt JE, Rink TJ. Journal of Biological Chemistry 1987;262:17362–17369. [PubMed: 3693357]
71. Di Virgilio F, Lew PD, Andersson T, Pozzan T. Journal of Biological Chemistry 1987;262:4574–4579. [PubMed: 2435712]
72. Huang Y, Putney JW. Journal of Biological Chemistry 1998;273:19554–19559. [PubMed: 9677379]
73. Franzius D, Hoth M, Penner R. Pflügers Arch 1994;428:433–438.
74. Schilling WP, Rajan L, Strobl-Jager E. Journal of Biological Chemistry 1989;264:12838–12848. [PubMed: 2546937]
75. Pittet D, Di VF, Pozzan T, Monod A, Lew DP. Journal of Biological Chemistry 1990;265:14256–14263. [PubMed: 1696945]
76. Lievremont JP, Bird GS, Putney JW. Am J Physiol Cell Physiol 2004;287:C1709–C1716. [PubMed: 15342342]
77. Putney JW Jr. Journal of Cell Science 2007;120:1959–1965. [PubMed: 17478524]
78. Liou J, Kim ML, Heo WD, Jones JT, Myers JW, Ferrell JE Jr, Meyer T. Curr Biol 2005;15:1235–1241. [PubMed: 16005298]

79. Roos J, DiGregorio PJ, Yeromin AV, Ohlsen K, Lioudyno M, Zhang S, Safrina O, Kozak JA, Wagner SL, Cahalan MD, Velicelebi G, Stauderman KA. Journal of Cell Biology 2005;169:435–445. [PubMed: 15866891]

80. Vig M, Peinelt C, Beck A, Koomoa DL, Rabah D, Koblan-Huberson M, Kraft S, Turner H, Fleig A, Penner R, Kinet JP. Science 2006;312:1220–1223. [PubMed: 16645049]

81. Feske S, Gwack Y, Prakriya M, Srikanth S, Puppel SH, Tanasa B, Hogan PG, Lewis RS, Daly M, Rao A. Nature 2006;441:179–185. [PubMed: 16582901]

82. Zhang SL, Yeromin AV, Zhang XH, Yu Y, Safrina O, Penna A, Roos J, Stauderman KA, Cahalan MD. Proc Natl Acad Sci U S A 2006;103:9357–9362. [PubMed: 16751269]

83. Wedel B, Boyles RR, Putney JW, Bird GS. J Physiol 2007;579:679–689. [PubMed: 17218358]

84. Liou J, Fivaz M, Inoue T, Meyer T. Proc Natl Acad Sci U S A 2007;104:9301–9306. [PubMed: 17517596]

85. Prakriya M, Feske S, Gwack Y, Srikanth S, Rao A, Hogan PG. Nature 2006;443:230–233. [PubMed: 16921383]

86. Yeromin AV, Zhang SL, Jiang W, Yu Y, Safrina O, Cahalan MD. Nature 2006;443:226–229. [PubMed: 16921385]

87. Vig M, Beck A, Billingsley JM, Lis A, Parvez S, Peinelt C, Koomoa DL, Soboloff J, Gill DL, Fleig A, Kinet JP, Penner R. Curr Biol 2006;16:2073–2079. [PubMed: 16978865]

88. Smyth JT, DeHaven WI, Bird GS, Putney JW Jr. Journal of Cell Science 2008;121:762–772. [PubMed: 18285445]

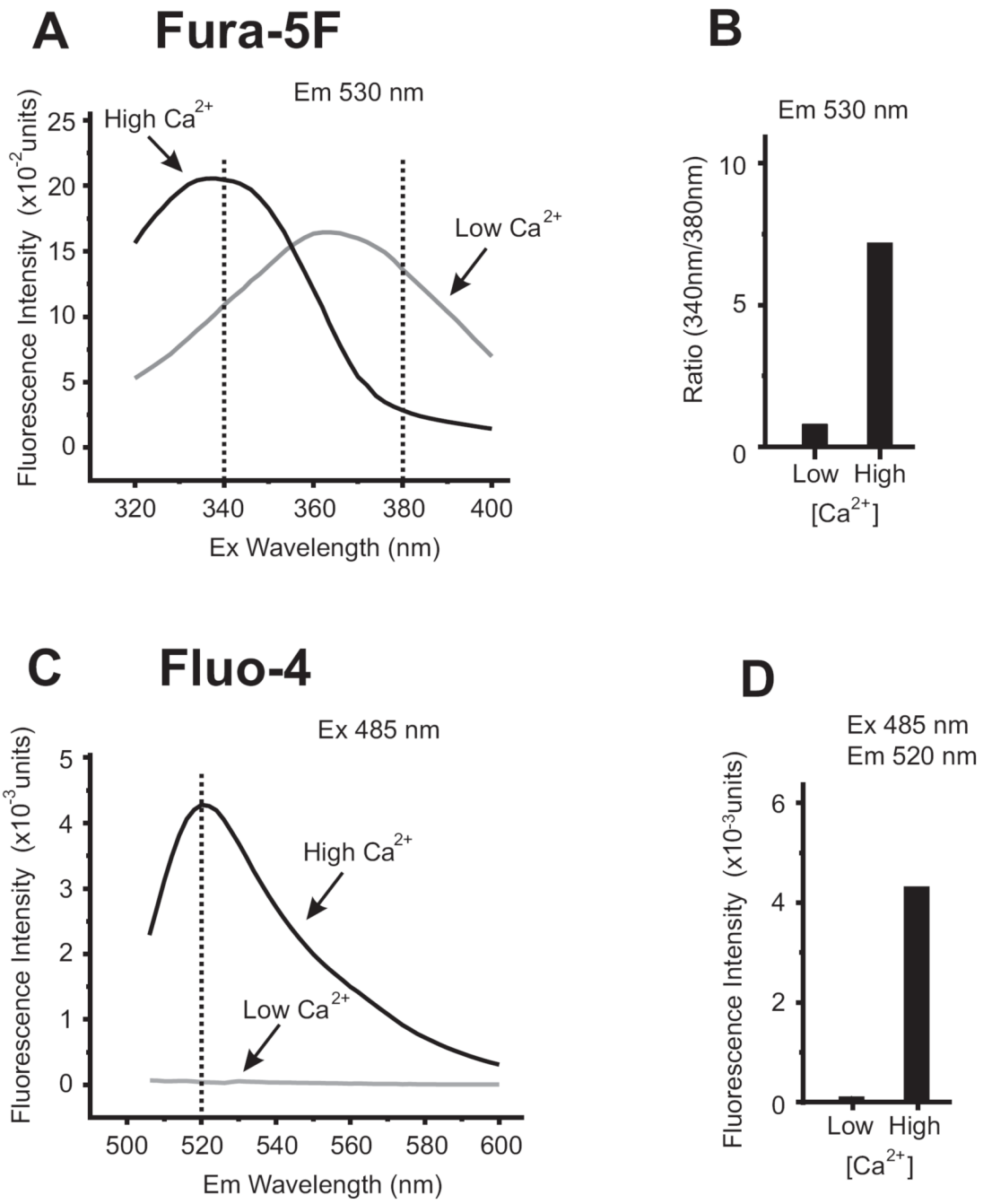

Figure. 1. Spectral Characteristic of Ratiometric and Single Wavelength Ca^{2+}Indicators

(A) Emission spectra of fura-5F (free-acid form) recorded at 530nm while scanning excitation wavelengths from 320-400nm. With 10 μM fura-5F dissolved in buffer containing 100 mM KCl, 20 mM HEPES, pH 7.2, switching between 'low Ca^{2+}' (buffer +200 μM BAPTA) and 'high Ca^{2+}' (buffer + 1 mM $CaCl_2$) conditions demonstrates the spectral shift characteristics of fura-5F. This [Ca^{2+}] change can be quantified by ratioing the emission fluorescence measured at 340nm and 380nm excitation wavelengths, as shown in **(B)**.

(C) Spectra for fluo-4 (free-acid form) was recorded with excitation at 485nm while scanning emission wavelengths from 500-600nm. Using the same buffers as in (A), switching between 'low Ca^{2+}'(buffer +200 μM BAPTA) and 'high Ca^{2+}' (buffer + 1 mM $CaCl_2$) demonstrates

the fluorescence intensity change in the spectra. This [Ca^{2+}] change can be quantified by selecting a single emission wavelength at which the intensity change is maximal, as shown in **(D)** (measured at 520nm).

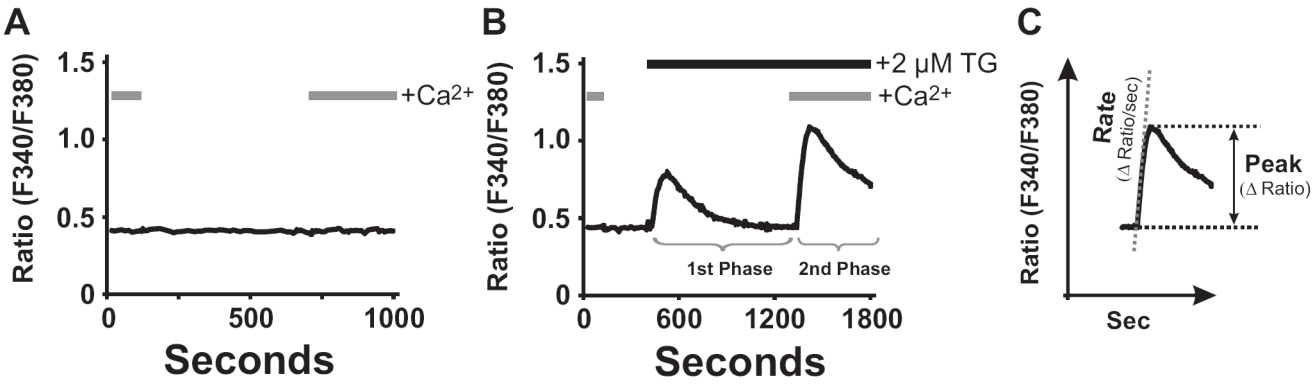

Figure. 2. 'Ca^{2+}re-addition' Protocol and Biphasic Ca^{2+}Signaling

HEK 293 cells were loaded with fura-5F and intracellular $[Ca^{2+}]_i$ measured as described in [57]. In **(A)** and **(B)**, HEK 293 cells were subjected to the 'Ca^{2+} re-addition' protocol by switching between buffer solutions with extracellular Ca^{2+} present or absent. In unstimulated HEK 293 cells **(A)**, the 'Ca^{2+} re-addition' protocol elicits no detectable change in $[Ca^{2+}]_i$. In **(B)**, the 'Ca^{2+} re-addition' protocol was combined with treatment of cells with a SERCA pump inhibitor (2 μM thapsigargin) to demonstrate a biphasic Ca^{2+} response. In the absence of extracellular $[Ca^{2+}]$, the transient first phase of intracellular Ca^{2+} release is observed. On 'Ca^{2+} re-addition', the seconds phase of SOCE is observed. As shown in **(C)**, the extent of SOCE activity can be quantified either as a rate of Ca^{2+} entry, or appeal response.

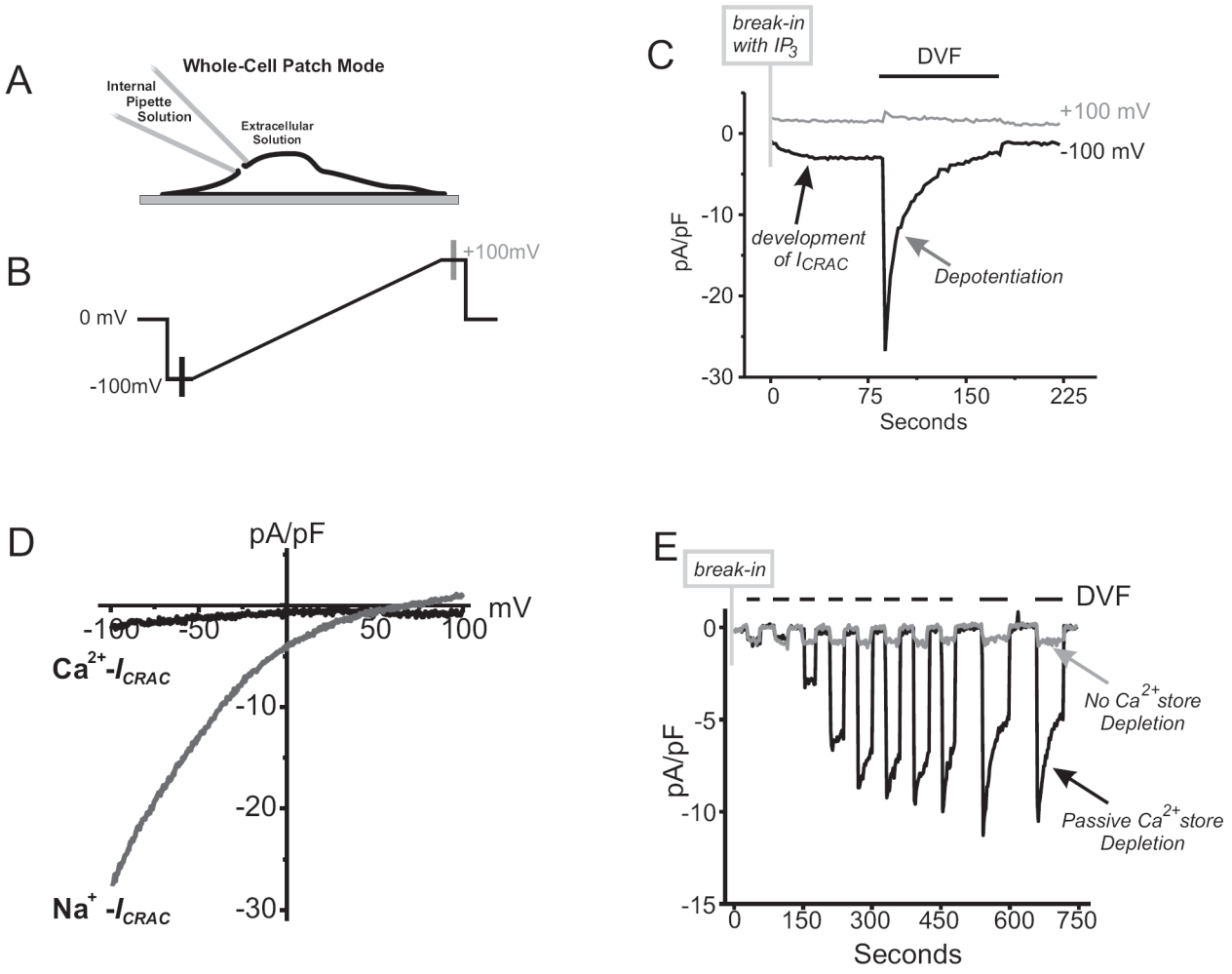

Figure 3. Biophysical Assessment of Store-Operated Currents

(A) Diagram showing the whole-cell configuration of the patch-clamp technique. As depicted, the use of this technique allows for access to the inside of the cell through the internal pipette solution (See Table 3 for example solutions), allowing for depletion of internal Ca^{2+} stores passively with BAPTA alone, or in combination with activating reagents such as IP_3.

(B) Schematic of a voltage ramp protocol used to assess store-operated Ca^{2+} currents. The protocol is repetitively applied over time, with 1 to 2 second intervals at 0 mV, to reveal currents develop during Ca^{2+} store depletion.

(C) An example I_{CRAC} in an RBL cell recorded using the protocol shown in panel B, and which was repetitively applied every two seconds. Internal Ca^{2+} stores were actively depleted by including 20 μM IP_3 and 10 mM BAPTA in the patch pipette solution. 10 mM Ca^{2+} was present in the external bathing solution. Following break-in with the patch pipette, a small (2 pA/pF) inward current develops at -100 mV, while no change is observed at +100 mV). Upon removal of all external divalent cations (divalent-free, DVF) in the extracellular media, Na^+ ions now permeate the store-operated channel to reveal Na^+-I_{CRAC}. Over time, Na^+-I_{CRAC} depotentiates, a process which is the reciprocal of a process known as Ca^{2+} dependent potentiation (CDP).

(D) Current-voltage relationship of Ca^{2+}-I_{CRAC} and Na^+-I_{CRAC} are inwardly rectifying Ca^{2+}- and Na^+-I_{CRAC} (data taken from recordings shown in panel C).

(E) In this whole-cell recording, DVF conditions were used to reveal I_{CRAC} in HEK 293 cells where, normally, Ca^{2+}- I_{CRAC} is difficult to detect. Following break-in, the protocol entails

switching the external bathing solutions between Ca^{2+} containing (10mM) and DVF bathing solutions. Using optimal conditions for passive depletion of Ca^{2+} stores (10 mM BAPTA in patch pipette solution), no I_{CRAC} is observed with 10mM Ca^{2+} in the external bathing solution. By switching to DVF conditions the developing Na^{+}-I_{CRAC} is revealed (black line trace). In contrast, supplementing the internal pipette solution with enough Ca^{2+} to "clamp" free Ca^{2+} at 100 nM (calculated using Maxchelator software; www.stanford.edu/~cpatton/maxc) prevents the passive depletion of Ca^{2+} stores upon break in, and no I_{CRAC} current develops (grey line trace) under all external bathing solution conditions.

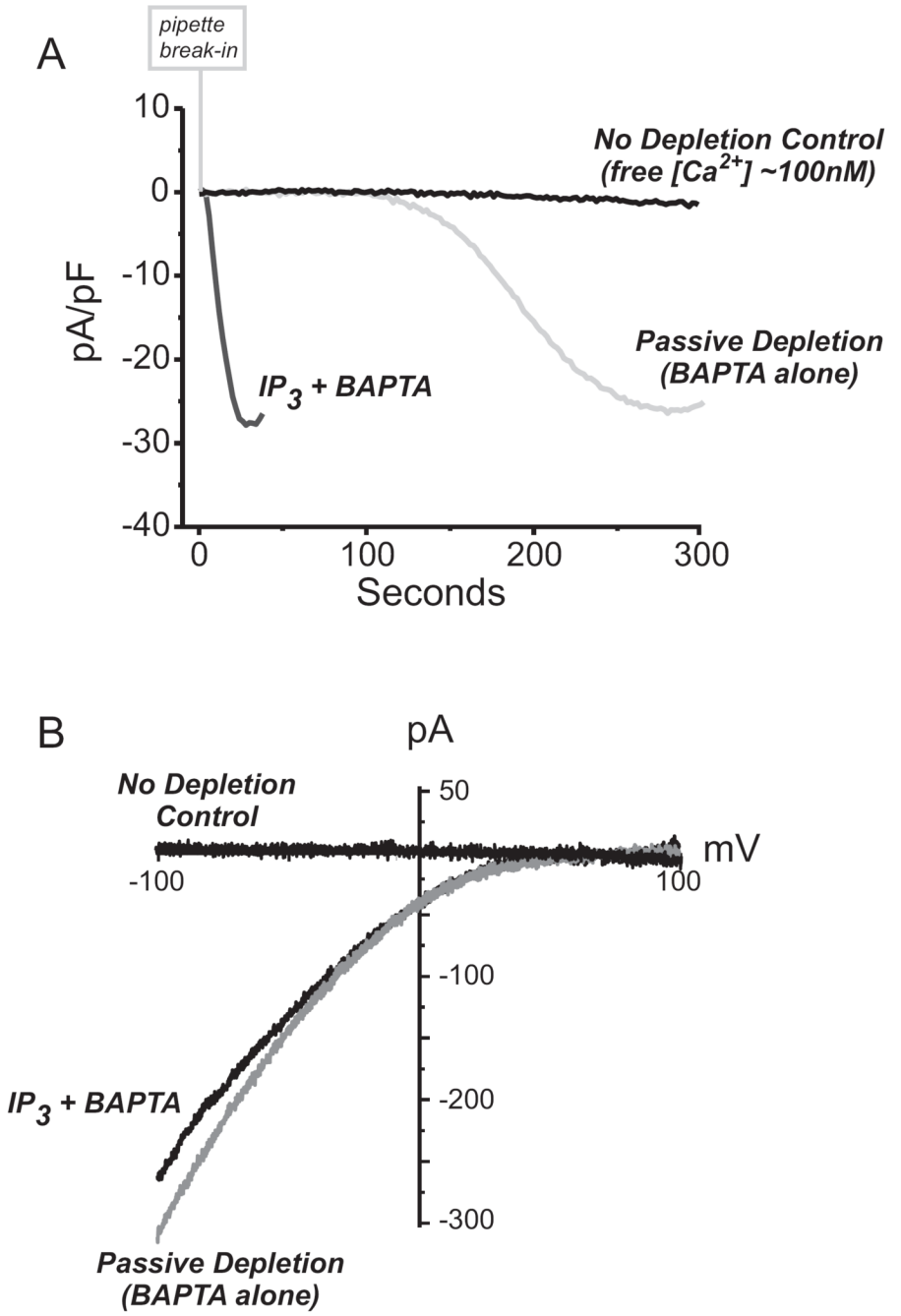

Figure 4. Methods for activating I_{CRAC}

(A) Whole –cell currents recorded in HEK 293 cells transfected with Stim1 and Orai1. From a holding potential of 0 mV, developing store-operated currents were recorded during voltage ramps (-100 mV to +100 mV) applied every two seconds using. This data shows a time course of Ca^{2+}-I_{CRAC} development recorded -100 mV. With coexpression of Stim1 and Orai1, "monster" Ca^{2+}-I_{CRAC} currents develop, and without the need to use DVF conditions. In this experiments, we compare the time course of Ca^{2+}-I_{CRAC} activation when Ca^{2+} stores are depleted passively (20mM BAPTA alone in the internal pipette solution) or actively (20mM BAPTA plus 20 μM IP_3 in the pipette). In contrast, "clamping" free [Ca^{2+}] in the internal

pipette solution to ~100 nM prevents Ca^{2+} store depletion, and no "monster" Ca^{2+}-I_{CRAC} is observed. In all recordings, the external [Ca^{2+}] was 10 mM.
(B) Current-voltage relationships for each of the "monster" Ca^{2+}-I_{CRAC} currents recorded in panel A are inwardly rectifying akin to endogenous I_{CRAC}.

Table 1

General Characteristics of Fura-5F and Fluo4

	Ratiometric	Ba^{2+}-entry	Mn^{2+}-quench	K_D (nM)
Fura-5F	Yes	Yes	Yes	400
Fluo-4	No	No	No	390

Table 2

Spectral and biological effects of Ca^{2+} and other ions on Ca^{2+} indicators and Ca^{2+} signaling processes.

	Ca^{2+}	Ba^{2+}	La^{3+}	Gd^{3+}	Mn^{2+}
Fura Signal	Yes	Yes	Yes	Yes	No
Fura Quench	No	No	No	No	Yes
Fluo-4 Signal	Yes	Poor	Yes	Yes	Poor
Fluo-4 Quench	No	No	No	No	No
Block SOCE	No	No	Yes	Yes	No
Substrate for PMCA/SERCA	Yes	No	?	?	No
Block PMCA	No	No	Yes	Yes	?

Table 3

Basic solutions for I_{crac} measurements

Extracellular Solutions (in mM)		
	Ca^{2+}-I_{crac}	**Na^{+}-I_{crac}**
NaCl	145	145
KCl	3	3
$MgCl_2$	2	0
Glucose	10	10
$CsCl_2$	10	10
EGTA	10	0
HEPES (pH 7.4)	0	0.1
Internal Pipette Solutions (in mM)		
	Passive Depletion	**No Depletion Control**
Cs Methansulfonate	145	145
$MgCl_2$	8	8
BAPTA	10	10
$CaCl_2$	0	3.5 (free $[Ca^{2+}]$ ~100nM)
HEPES (pH 7.2 with CsOH)	10	10

Note: High $[Mg^{2+}]$ required to block MIC currents [43].

Free $[Ca^{2+}]$ calculated using MaxChelator (www.stanford.edu/~cpatton/maxc)